

SMOS Daily Polar Gridded Brightness Temperatures (L3B)

Xiangshan Tian-Kunze, Lars Kaleschke, Nina Maass, and Amelie Schmitt
Institute of Oceanography, KlimaCampus, University of Hamburg, Germany

December 8, 2016

Revision history

Date	Author	Comments
Dec 20, 2012	X. Tian-Kunze	first draft
Dec 5, 2016	X. Tian-Kunze	revision

Contact address+ Emails

SMOS Sea Ice scientist
Dr. Xiangshan Tian-Kunze
Institute of Oceanography
University of Hamburg
Bundesstrasse 53, 20146 Hamburg, Germany

Principal investigator:
Prof. Dr. Lars Kaleschke
Institute of Oceanography
University of Hamburg
Bundesstrasse 53, 20146 Hamburg, Germany

ICDC
Dr. Stefan Kern
University of Hamburg
Grindelberg 5, 20144 Hamburg, Germany

Contents

1	Introduction	4
2	L1C Brightness Temperature	4
3	L3B Brightness Temperature	6
3.1	RFI, geophysical noise, and data loss	7
3.1.1	Data filtering: threshold method used in v2.1	9
3.1.2	Data filtering: flag-based method used in v3.1	12
3.2	L3B TB difference caused by the transition from v505 to v620 in L1C data	14
3.3	TB uncertainty	15
4	Operational processing steps from L1C to L3B TB	16
5	Data description	16
6	References	19

1 Introduction

The Microwave Imaging Radiometer with Aperture Synthesis (MIRAS) on board of European Space Agency's (ESA) Soil Moisture and Ocean Salinity (SMOS) mission measures Earth's radiation at a frequency of 1.4 GHz (L-band). Brightness temperatures are measured in full polarization and incidence angles ranging from 0° to 65° . Compared to other sensors which operate at higher frequencies, L-band radiometry has the advantage of a large penetration depth inside the sea ice. It has global coverage every three days (Kerr et al., 2001), whereas daily coverage up to 85° latitude is archived in the polar regions. The spatial resolution varies from about 35 km at nadir view to more than 50 km at higher incidence angles. Although originally designed for the observation of soil moisture and ocean salinity, an important application of SMOS brightness temperatures in the polar regions is to derive the sea ice thickness. (Kaleschke et al., 2010, 2012; Tian-Kunze et al., 2014; Huntemann et al., 2014; Maaß et al., 2015) have demonstrated the possibility of sea ice thickness retrieval from SMOS brightness temperatures.

In this document, we will describe the SMOS L3B brightness temperature data set, which is the basis of SMOS sea ice thickness retrieval at the university of Hamburg. The updates from v2.1 L3B data to v3.1 L3B data will be highlighted.

2 L1C Brightness Temperature

During the SMOS commissioning phase (from November 2009 to May 2010), the antenna's dual and full mode measurements are tested. Therefore, either dual mode or full mode L1C data were available in this phase, with daily data partly or completely missing in some days. After the SMOS mission went to the operational phase, only full mode data have been available (about 9 GB per day for ocean product). Browse products with incidence angle 43° are

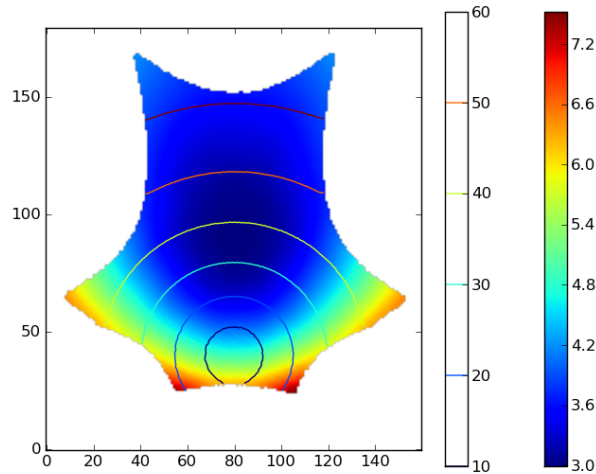


Figure 1: Distribution of radiometric accuracy ([K]) within a typical snapshot with incidence angles as contour lines ([degree]). The snapshot is gridded with 10 km spatial grid resolution (axis unit).

delivered separately. L1C data are swath-based and include information about snapshot ID, polarization, incidence angles, geometric and Faraday rotation angles. Ocean and land products are stored separately. For our purpose, however, we use only ocean product. L1C data are downloaded from ESADPGSFTP server.

A typical SMOS snapshot has a spatial dimension of about 1500 km x 1500 km. The geometric distribution of incidence angles and radiometric accuracy within a snapshot is shown in Figure 1.

Although the earth surface is seen by SMOS snapshotwise, SMOS L1C data are not sorted by snapshots but by the so called DGG grid points. The brightness temperatures at the grid points are calculated with an image reconstruction (Kerr et al., 2001). DGGs are Fixed Earth Grid coordinates of the ISEA 4-9 hexagonal grid centers which are distributed into ten corresponding zones with 262145 grid points in each zone (Indra, 2010). The spatial distance of two ISEA grids is about 15 km.

The version number of L1C brightness temperature has changed several times. The version numbers and their periods are listed in the Table 1. Sea ice thickness (with data version v3.1) retrieved with Algorithm III is based on the v620 L1C data.

Table 1: Overview of SMOS L1C data

Data version	Mode	Time period	Remarks
v330	Dual	Dec.12 and 13, 2009; Mar. 5 and 7, 2010	
v344	Full	Jul. 19, 2010- Dec. 26, 2011	
v346	Dual, Full	Jan. 12, 2010- May 23, 2011	
v346	Full	May 24, 2010- Oct. 23, 2011	
v503	Full	Oct. 23, 2011- Nov. 2011	
v504	Full	Nov. 2011-Mar.21, 2012	
v505	Dual, Full	Jan. 12, 2010-now	reprocessed for the whole period
v620	Dual, Full	Jan. 12, 2010-now	reprocessed for the whole period

3 L3B Brightness Temperature

Level 3 SMOS brightness temperature data (henceforth called L3B TB) are processed at the university of Hamburg on daily basis. All orbital data for each 24-hour period are collected at the respective SMOS ISEA grids in both polar regions with latitude higher than 50°. No single swath-based Level 2 dataset is produced in our processing chain but all information is stored in an intermediate Level 3A file to enable an easy reprocessing. The Level 3A file is not intended for distribution but only for internal processing.

Brightness temperatures used in the SMOS sea ice thickness Al-

gorithm I, II, II*, and III are the daily mean intensities averaged over incidence angles from 0° to 40° . The intensity is the average of horizontally and vertically polarized brightness temperatures:

$$I = (TB_h + TB_v)/2, \quad (1)$$

Although the horizontally and vertically polarized brightness temperatures vary with incidence angles, the intensity remains almost constant in this incidence angle range over sea ice (Fig. 2). By using the whole incidence angle range of 0 - 40° , we can get more than 100 brightness temperature measurements per grid point per day for the main part of the Arctic Ocean (Figure 3). The radiometric accuracy of single brightness temperature measurement is larger than 3 K. By averaging over numerous measurements we can reduce the brightness temperature uncertainty to about 0.5 K. However, by averaging, we partly reduce the geophysical and temporal variability. The daily averaged brightness temperature intensities in the Arctic and Antarctic are interpolated with a nearest-neighbor algorithm and gridded into the “National Snow and Ice Data Center (NSIDC)” polar stereographic projection with a grid resolution of 12.5 km. We call this gridded daily mean brightness temperature as L3B SMOS TB data.

3.1 RFI, geophysical noise, and data loss

The SMOS measurements are partly influenced by the Radio Frequency Interference (RFI) which comes from radar, TV and radio transmission at the protected L-band electromagnetic spectrum (1400-1427 MHz) at which the SMOS radiometer operates (Camps et al., 2010). The detection of the RFI sources and the mitigation of RFI influence are critical steps for the further retrieval of geophysical parameters. The RFI influence depends on the incidence angle, polarization, and ascending and descending modes of the satellite (Camps et al., 2010). At near nadir look RFI signals have smaller impact on

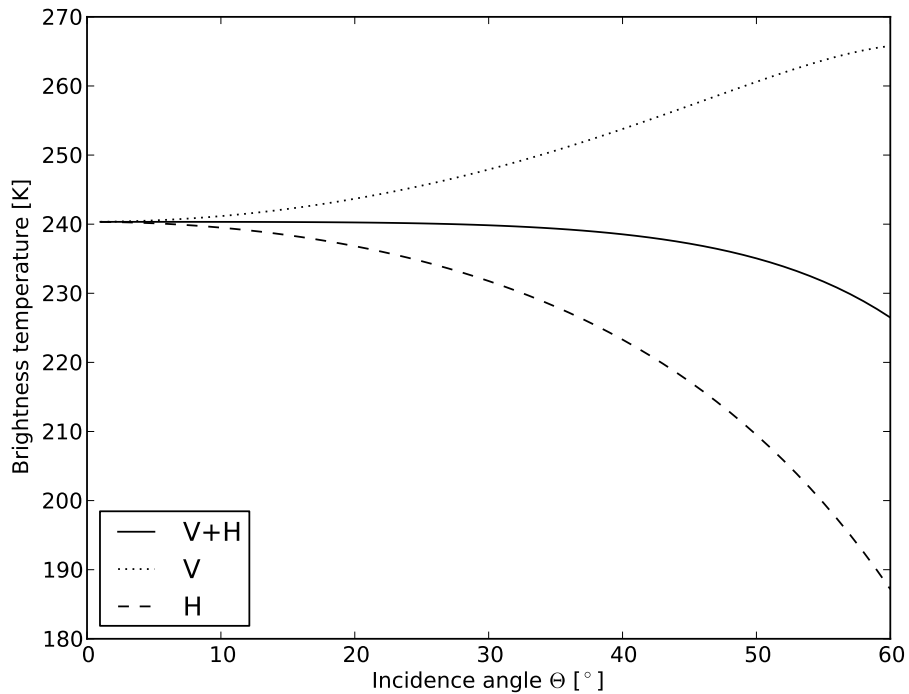


Figure 2: Vertically (V) and horizontally (H) polarized components of the brightness temperatures and the first Stokes parameter I as a function of incidence angle calculated using a three layer model for sea ice with a thickness of $d = 1\text{m}$, salinity $S = 8\text{ g/kg}$, and temperature $T = -7^\circ\text{C}$.

the surrounding regions than at higher incidence angles.

3.1.1 Data filtering: threshold method used in v2.1

A closer look into RFI contaminated snapshots shows that due to the image reconstruction RFI can either completely or partly destroys a snapshot. In the v2.1 L3B TB data, we applied a threshold value for both horizontally and vertically polarized brightness temperatures. If either of them exceeds 300 K in one snapshot, this snapshot is considered as RFI contaminated. Brightness temperature higher than 300 K is not realistic both in the Arctic and Antarctic regions over the year.

RFI influence is seldom observed in the Antarctic. However, in the Arctic RFI contamination is widely and frequently detected. To get an overview of the number of available TB measurements, we compared at each grid point daily averaged total number of TB measurements, as well as the number of “good” TB measurements without RFI (as long as it is not detected by our RFI filter). The time period used here is from 2010.10.01 to 2010.12.26, in which the RFI contamination is relatively strong. v505 L1C data are used. As Figure 3 shows, in average there are more than 200 SMOS measurements per day at each grid point in most regions of Arctic. Strongly RFI affected regions are for example the region northeasterly from Greenland and part of Canadian Arctic Archipelago. Due to the efforts of ESA and corresponding countries, RFI has been reduced strongly since the launch of SMOS. Figure 4 shows the comparison of data loss caused by RFI from 2010 and 2011. The data loss is defined as the ratio of the number of RFI contaminated measurements to the total number of measurements.

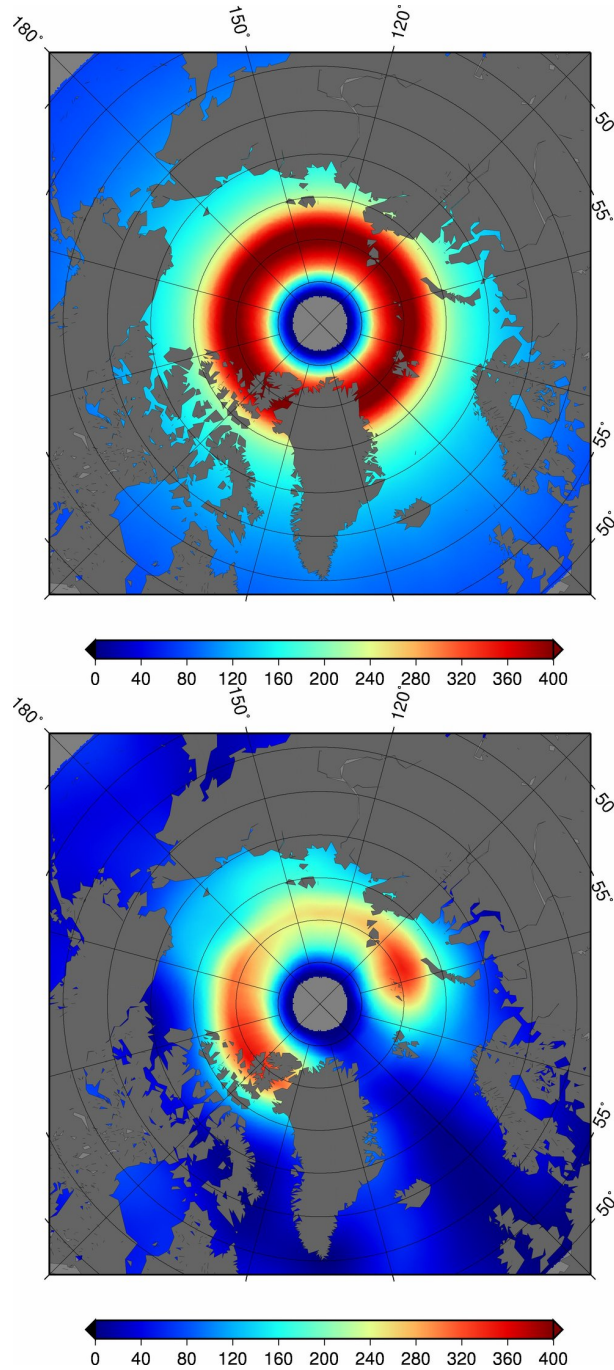


Figure 3: The number of total and “good” measurements per day. top: total bottom: only from ‘good’ snapshots without RFI detected by our RFI filter. Time period 2010.10.01- 2010.12.26, Incidence angle: 0°-40°, v505 L1C data are used.

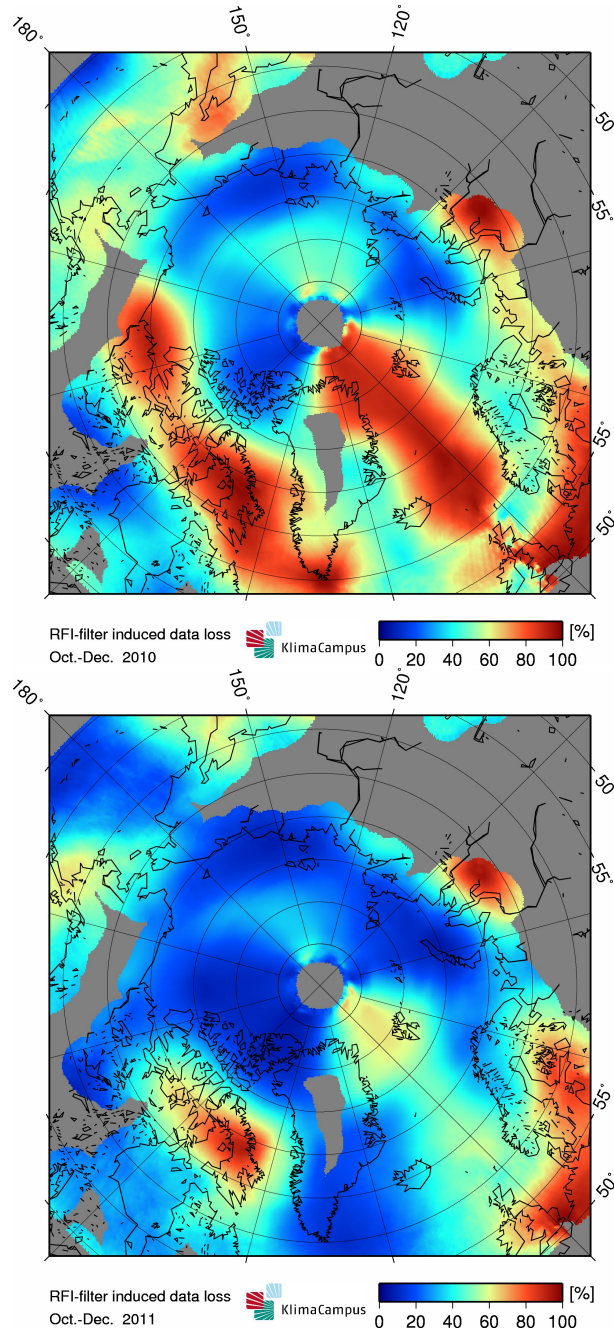


Figure 4: Brightness temperature data loss caused by RFI for the period of 2010.10.01- 2010.12.26 averaged over incidence angles 0° - 40° , v505 L1C data are used.

3.1.2 Data filtering: flag-based method used in v3.1

In the sea ice thickness retrieval Algorithm I, II and II*, we implemented the simple threshold method to filter out the “bad” TB measurements. This leads to considerable data loss, especially in the Barents Sea, Laptev Sea, East Siberian Sea, and north of Greenland. RFI flagging (Table 2 and Table 3) in the L1C data has been improved distinctly in the new reprocessed 620 version. A thorough analysis has been done within SMOS + Sea Ice project (ESA ESTEC Contract No.: 4000101476/10/NL/CT) to compare the implementation of combined RFI flagging provided in the v620 L1C data with that of simple threshold method used until now (see more details in SMOS + Sea Ice TR1 UHH section 2.1).

Table 2: RFI flags in the SMOS v620 L1C product.

RFI flags	
TBH/TBX RFI flag	Snapshot is contaminated with RFI in H polarisation
TBV/TBY RFI flag	Snapshot is contaminated with RFI in V polarisation
Point source RFI flag	Pixel is affected by point source RFI
Tail RFI flag	Pixel is affected by the tails of a point source RFI

Table 3: Other flags in the SMOS v620 L1C product.

Other flags	
Sun point flag	Pixel is located in a zone where a sun alias was reconstructed
Sun tails flag	Pixel is located in the hexagonal alias directions centred on a sun alias
Sun glint area flag	Pixel is located in a zone where sun reflection has been detected
Moon point flag	Pixel is located in a zone where a moon alias was reconstructed
Border field of view flag	Pixel is close to the border delimiting the extended alias free zone or to the unit circle replicas borders

The analysis has shown that the new SMOS flags in v620 detect a large part of data that is contaminated by RFI or by sun or

by geometric effects. Especially for point sources, these flags have an advantage over the threshold method, because they only flag the actual source and thus, the rest of the uncontaminated values in the snapshot do not have to be discarded. By using a combination of the SMOS flags for point and tail RFI, and sun point alias with a subsequent application of the old threshold method to remove all remaining values larger than 300 K, we can have more TB measurements to average, which will reduce the uncertainty of daily TB mean. In this new method it is possible that contaminated pixels with values smaller than 300 K might not be detected. This small disadvantage is, however, outweighed by the large number of advantages of the new method. With the new method the overall data loss is reduced, the occurrence of data holes in the Central Arctic is largely prevented (Fig. 5), and geometric stripes caused by sun aliases are diminished. Therefore, this new flagging method is implemented in the Algorithm III.

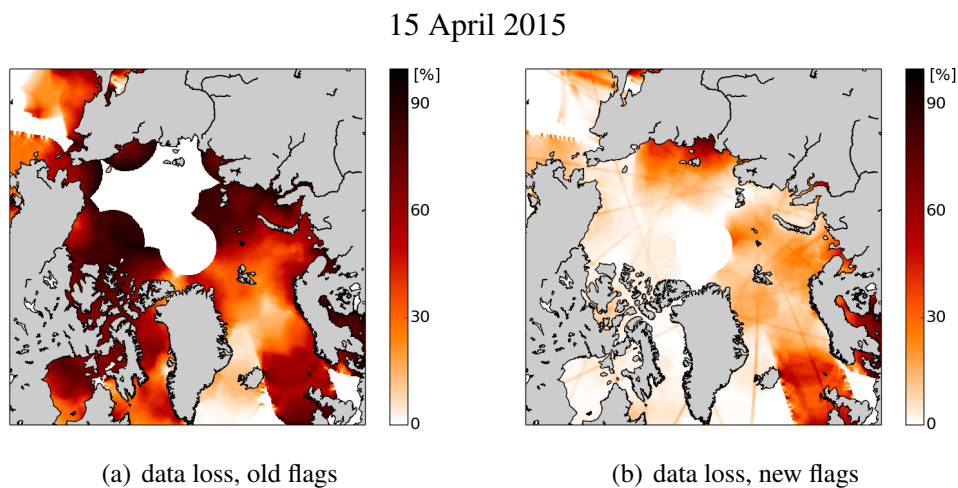


Figure 5: Data loss on 15 April 2015 using the old UHH flags (left) and the new combined method (right).

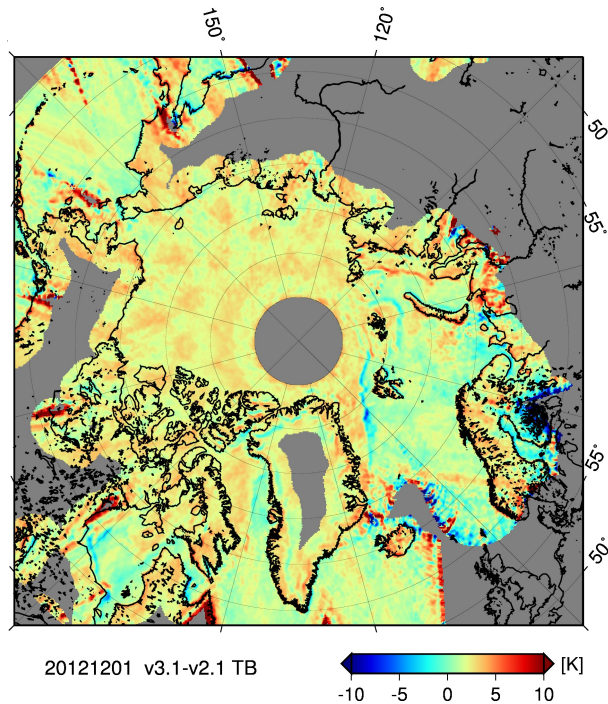


Figure 6: L3B TB difference between v3.1 and v2.1 on December 1, 2012. The main difference is caused by the transition of L1C data version from v505 to v620.

3.2 L3B TB difference caused by the transition from v505 to v620 in L1C data

ESA changed the L1C product version from 5.05 to 6.20 starting on May 5, 2015. Though v3.1 L3B TB data are reprocessed consistently using v620 L1C data, first released v2.1 L3B TB data were based on v505 L1C data until May 4, 2015. Fig. 6 shows the TB difference between v3.1 (which is based on v620 L1C data) and v2.1 (which is based on v505 L1C data). The brightness temperatures in v620 L1C data is on average about 3K higher than v505 data, however, the difference depends on the region and time.

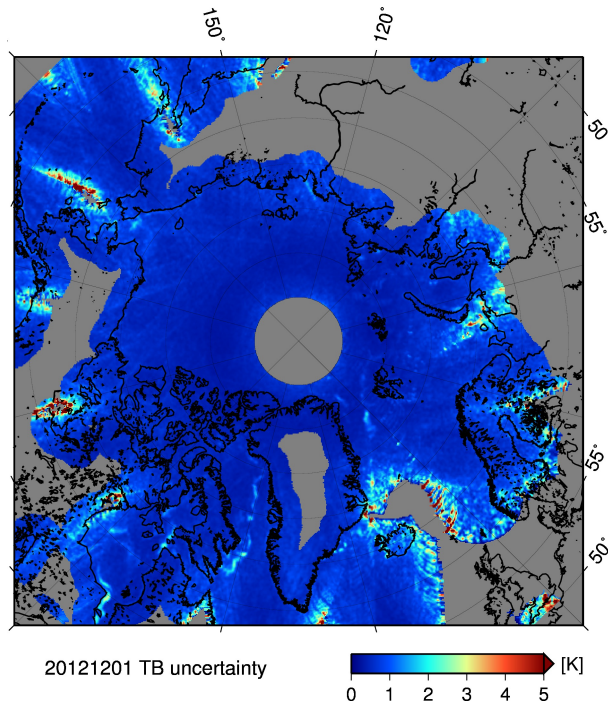


Figure 7: TB uncertainty in v3.1 data for December 1, 2012 in the Arctic.

3.3 TB uncertainty

An estimation of uncertainties of brightness temperatures is provided at each grid point on daily basis in our data set. The uncertainties of brightness temperatures are caused not only by the radiometric accuracy of the instrument which is dependent on the incidence angles, but also the variability of the measurements from consecutive snapshots and from different swaths. We define the brightness temperature uncertainty as one standard deviation divided by the square root of the number of TB_h and TB_v pairs (nPair) used for the calculation of mean daily intensity. Standard deviation reflects the variability of brightness temperature measurements. An example of brightness temperature uncertainty distribution for 2012.12.01 is shown in Figure 7.

4 Operational processing steps from L1C to L3B TB

The operational processing steps from L1C to L3B are shown in Figure 8. The processing steps from L1C to L3 are optimized to ease the reprocessing after possible revisions of the filters and retrieval algorithms. For this purpose we produce an intermediate L3A product. The daily L3A data collects all orbital data for each 24-hour period at the respective DGG grid points. The daily L3A product is stored in north and south polar regions separately and contains not only all the daily available brightness temperature measurements but also incidence angle, polarization and flags, Snapshot ID, Faraday and geometric rotation information. The L3A product is stored in HDF format and can be read in a few seconds. L3B product which includes the first Stokes component, uncertainties, as well as the number of TB_h and TB_v pairs and the data loss percentage caused by RFI, is derived from L3A product. The processing chain from L1C to L3B data runs in a semi-automatic way with 24 hours latency.

5 Data description

The variables TB, TB uncertainty, nPair, and RFI ratio have dimensions of (time,y,x), with (y=896 x=608) in the Arctic and (y=664 x=632) in the Antarctic. The time is the hours since 2010-01-01 00:00:00. Geolocations (latitude and longitude) are given at each grid cell. An overview of the variables is given in Table 4.

Table 4: Description of variables

variables	long name	data type	dimension	missing value	scale factor	unit
Latitude	latitude	32 bit float	(y,x)	-999	1.0	degree
Longitude	longitude	32 bit float	(y,x)	-999	1.0	degree
TB	brightness temperature intensity (TBh+TBv)/2	32 bit float	(time,y,x)	-999	1.0	K
TB uncertainty	brightness temperature uncertainty	32 bit float	(time,y,x)	-999	1.0	K
nPair	number of TBh and TBv pairs	16 bit integer	(time,y,x)	-999	1.0	
RFI ratio	percent of RFI- contaminated measurements in total measurements	32 bit float	(time,y,x)	-999	1.0	percent

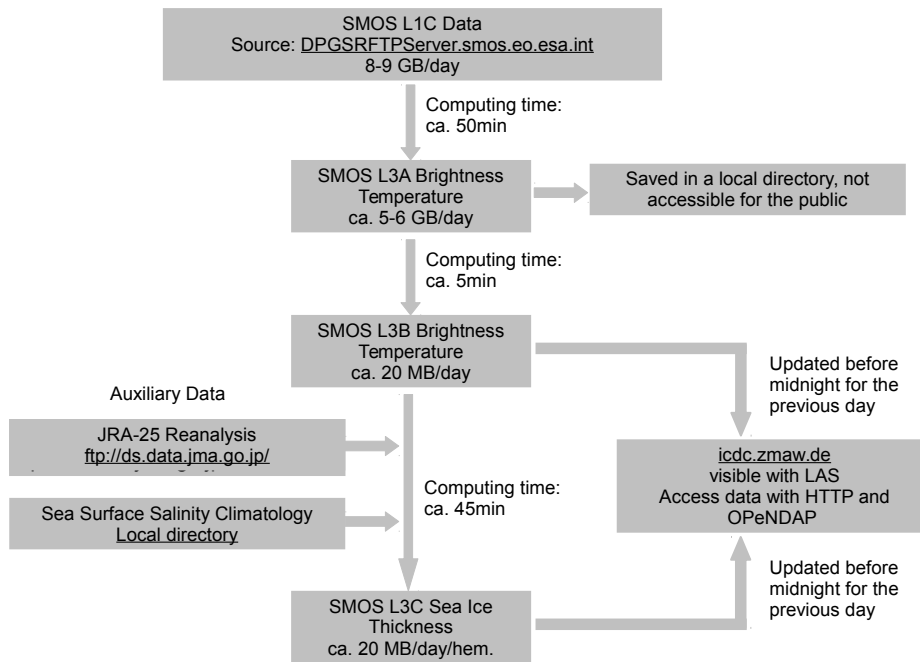


Figure 8: The flow chart of processing steps from SMOS L1C to L3

Missing data:

Due to anomalies related to the temperature readings on one of the antenna segments of arm B, between 27 and 31 Dec. 2010 no data are available. Between 14 and 16 March, 2016, data are missing (partly or completely) due to a major SW upgrade onboard SMOS.

File and Directory Structure:

Data files are offered on the THREDDS server. A quick look of daily data can be visualized with LAS. Data are available since 2010.01.12 daily in NetCDF format for the north and south polar regions.

Data citation:

The following example shows how to cite the use of this data set

in a publication.

X. Tian-Kunze, L. Kaleschke, N. Maass, and A. Schmitt (2016) SMOS Daily Polar Gridded Brightness Temperatures (L3B), [list dates of temporal coverage used]. ICDC, University of Hamburg, Germany, Digital media.

6 References

References

- Camps, A., Gourrion, J., Tarongi, J., Gutierrez, A., Barbosa, J., and Castro, R.: RFI Analysis in SMOS Imagery, in: Geoscience and Remote Sensing Symposium (IGRASS proceedings 2010, pp. 2007–2010, 2010.
- Huntemann, M., Heygster, G., Kaleschke, L., Krumpen, T., Mäkyänen, M., and Drusch, M.: Empirical sea ice thickness retrieval during the freeze up period from SMOS high incident angle observations, *The Cryosphere*, 8, 439–451, 2014.
- Indra: SMOS DPGS: SMOS Level 1 and Auxiliary Data Products Specifications, Ref. SO-TN-IDR-GS-0005, 2010.
- Kaleschke, L., Maass, N., Haas, C., Heygster, S., and Tonboe, R.: A sea ice thickness retrieval model for 1.4 GHz radiometry and application to airborne measurements over low salinity sea ice, *The Cryosphere*, 4, 583–592, doi:{10.5194/tc-4-583-2010}, 2010.
- Kaleschke, L., Tian-Kunze, X., Maaß, N., Mäkyänen, M., and Drusch, M.: Sea ice thickness retrieval from SMOS brightness temperatures during the Arctic freeze-up period, *Geophys. Res. Lett.*, doi:{10.1029/2012GL050916}, 2012.
- Kerr, Y., Waldteufel, P., Wigneron, J., Martinuzzi, J., Font, J., and Berger, M.: Soil moisture retrieval from space: The Soil Mois-

ture and Ocean Salinity (SMOS) mission, *IEEE Transactions on Geoscience and Remote Sensing*, 39, 1729 – 1735, 2001.

Maaß, N., Kaleschke, L., Tian-Kunze, X., Mäkynen, M., Drusch, M., Krumpfen, T., Hendricks, S., Lensu, M., Haapala, J., and Haas, C.: Validation of SMOS sea ice thickness retrieval in the northern Baltic Sea, *Tellus A*, 67, 2015.

Tian-Kunze, X., Kaleschke, L., Maaß, N., Mäkynen, M., Serra, N., Drusch, M., and Krumpfen, T.: SMOS-derived thin sea ice thickness: algorithm baseline, product specifications and initial verification, *The Cryosphere*, 8, 997–1018, 2014.